

# Vision-TTT: Efficient and Expressive Visual Representation Learning with Test-Time Training

Quan Kong<sup>1</sup>, Yanru Xiao<sup>2</sup>, Yuhao Shen<sup>1</sup>, and Cong Wang<sup>1</sup>

<sup>1</sup>  Zhejiang University, Hangzhou, China

<sup>2</sup>  Amazon Web Services, USA

{qkv, riven, cwang85}@zju.edu.cn

yxiao002@odu.edu

**Abstract.** Learning efficient and expressive visual representation has long been the pursuit of computer vision research. While Vision Transformers (ViTs) gradually replace traditional Convolutional Neural Networks (CNNs) as more scalable vision learners, their applications are plagued by the quadratic complexity of the self-attention mechanism. To address the challenge, we introduce a new linear-time sequence modeling method Test-Time Training (TTT) into vision and propose Vision-TTT, which compresses the visual token sequence in a novel self-supervised learning manner. By incorporating bidirectional scan strategy and the Conv2d module, Vision-TTT effectively extends vanilla TTT to model 2D visual correlations with global receptive fields. Extensive experiments show that `Vittt-T/S/B` achieve 77.3%, 81.2%, 82.5% Top-1 accuracy on ImageNet classification and also greatly outperform their counterparts on downstream tasks. At  $1280 \times 1280$  resolution, `Vittt-T` reduces FLOPs by 79.4% and runs  $4.38 \times$  faster with 88.9% less memory than DeiT-T. These results demonstrate the expressiveness and efficiency of Vision-TTT as a strong candidate for the next-generation generic visual backbone. Codes are available at <https://github.com/imKQv/Vittt>.

**Keywords:** Visual representation learning · Linear Complexity Visual Sequence Modeling · Test-Time Training

## 1 Introduction

Learning efficient and expressive visual representation learning has long been a fundamental task in computer vision research. Convolutional Neural Networks (CNNs) [22, 24, 42, 46, 47, 52, 58] represent classic architectures in this domain. They can efficiently capture spatial hierarchies, yet are limited by the static nature of convolutional kernels, which restricts their performance scalability. In recent years, Vision Transformers (ViTs) [2, 13, 17, 33, 50, 63, 66] have explored the self-attention mechanism for visual sequence modeling. With superior scalability demonstrated on large-scale experiments [38, 41], ViTs have gradually become a standard architectural paradigm in both academia and industry.

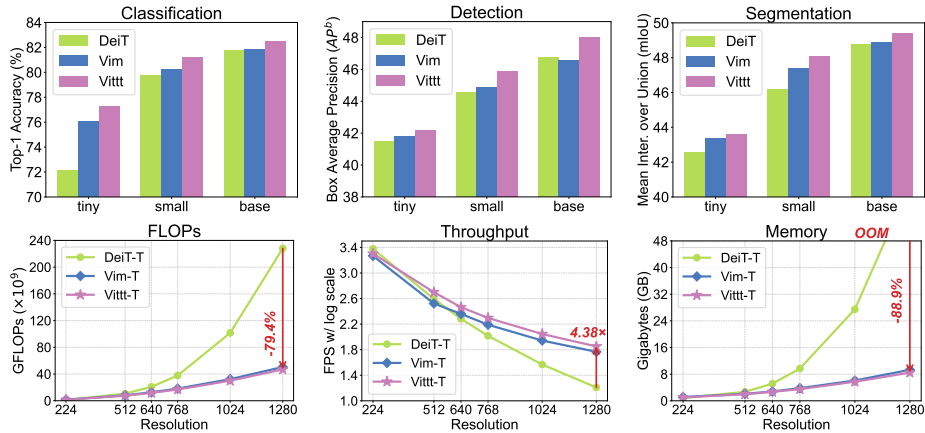


**Fig. 1:** Performance and efficiency comparison between DeiT [50], Vim [67] and our Vittt model. Results show that Vittt not only achieves superior performance on ImageNet classification and downstream detection and segmentation tasks, but also is more computation and memory efficient in dealing with high-resolution images.

However, as the community’s demand for high-resolution image understanding continues to grow, ViTs are severely plagued by their quadratic computational complexity [51] when processing long-sequence tasks. To tackle this bottleneck, researchers have been striving to pursue a Pareto-optimal architecture that balances expressiveness and efficiency. Among the emerging visual sequence models [14,20,28,32,67], Vision-Mambas [32,67] represent the most popular and representative approaches that build upon the State Space Models (SSMs) with selective scan design and hardware-aware parallelism [7,18].

In this paper, we build on a new linear-time sequence modeling paradigm Test-Time Training (TTT) [44] and propose the Vision-TTT architecture, which establishes a new Pareto front between the expressiveness and efficiency in visual representation. In the context of visual sequence modeling [13,14,28,67], the core idea of TTT is to treat the visual token sequence of an image as a data stream, along which self-supervised learning is performed to compress visual semantics into a hidden state via gradient updates. As a result, the token semantics are explicitly guided by the gradients to form an expressive and explainable visual representation. Furthermore, linear-complexity efficiency can also be achieved through hardware-aware matrix multiplication parallelism [44].

Despite this, vanilla TTT is originally designed for unidirectional modeling with inherent temporal dependence. This renders its global perception capability advantages in NLP inadequate for fully global modeling in visual tasks. To introduce spatial locality, we incorporate long-term bidirectional scanning [39] and short-term Conv2d operations [5] with negligible extra parameters. Benefiting from these architectural designs, Vision-TTT exhibits a globally radial Effective Receptive Field (ERF) [35] to construct representations with explicit 2D correlations. As shown in Fig. 1, Vittt greatly outperforms strong baselines

of DeiT [50] and Vim [67] on both classification and downstream tasks, while keeping linear computational and memory complexity for high-resolution images.

The main contributions of this paper are summarized as follows:

- ✧ We propose Vision-TTT, the first generic visual backbone to leverage Test-Time Training mechanism with gradient-driven state adaptation to capture visual semantics and build expressive visual representations.
- ✧ By integrating hardware-aware kernel implementation, Vision-TTT alleviates the quadratic complexity bottleneck of Vision Transformers and achieves linear complexity modeling. At  $1280 \times 1280$  resolution, `Vittt-T` saves 79.4% FLOPs and runs 4.38 $\times$  faster with 88.9% less memory than DeiT-T.
- ✧ With a dedicated 2D architectural design, Vision-TTT expands vanilla TTT to visual representation tasks with spatial locality. Extensive experiments show that `Vittt-T/S/B` achieve 77.3%, 81.2%, 82.5% Top-1 accuracy on ImageNet classification, and significantly outperform their counterparts on downstream COCO detection and ADE20K segmentation tasks.

## 2 Related Work

**Visual Representation Learning.** Visual representation Learning serves as the foundation for a wide range of computer vision tasks [9,29,65]. It has evolved into two mainstream paradigms, convolution-based method and visual sequence modeling. Convolutional Neural Networks (CNNs) [11, 22, 24, 27, 31, 34, 42, 46, 47, 52, 54, 60] have long been the dominant architecture in this field due to their efficiency in processing spatial vision data. However, CNNs are limited by the static nature of convolution kernels [15], which restricts their scalability in performance. In recent years, Vision Transformer (ViT) [13] has pioneered the paradigm of visual sequence modeling, and DeiT [50] further refines ViT with advanced training techniques and distillation. They ignite a series of follow-up works that incorporate hierarchical designs [10, 12, 48, 55, 63, 64, 66] or dedicated convolution operations [6, 17]. Despite their remarkable performance, ViTs suffer from the quadratic complexity of the self-attention mechanism [51] when dealing with high-resolution images.

**Linear Complexity Visual Sequence Modeling.** To pursue linear complexity representation, various RNN-like sequence models [18, 37, 44, 62] have attracted growing interest. Building upon State Space Models (SSMs) [7, 18, 19], Vim [67] and VMamba [32] focus on employing 2D scanning strategies to gain global perception. Their variants [3, 25, 36, 61] mainly improve the efficiency-expressiveness trade-off via visually-adapted SSMs, while MambaVision [20] adopts a hybrid architecture of SSM and SwinTransformer [33] blocks for local-to-global perception. In addition, Vision-RWKV [14] introduces temporal decay to capture long-range dependency and ViG [28] adopts gated linear attention [62] to enhance expressiveness. Nevertheless, the impact of Test-Time Training (TTT) [44] for generic visual representation learning still remains under-explored.

**Test-Time Training.** The early multi-task learning version of TTT [45] introduces an auxiliary self-supervised task parallel to the main task, aiming to ad-

dress the distribution shift problem on test images. It has been further extended to video stream processing [53] and object detection [16]. Recently, TTT [44] has been revisited under a meta-learning [1] perspective for adaptive sequence modeling, which involves an inner loop for self-supervised reconstruction and an outer loop for the main task [43,59]. **Our work focuses on the meta-learning formulation of TTT [44]** as an RNN-like visual sequence modeling approach to learn efficient and expressive visual representations.

### 3 Preliminary

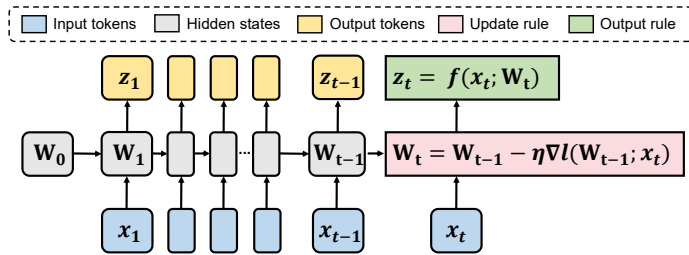


**Fig. 2:** Basics of TTT. The core idea is to update the hidden state  $W$  with steps of self-supervised gradient descent and then forward the output to the next layer.

Similar to most recurrent models like LSTM [23], Mamba [18] and RWKV [37], TTT is also a special RNN that maintains a hidden state  $W \in \mathbb{R}^{D \times D}$  and follows an update rule and an output rule. As illustrated in Fig. 2, the core idea is to treat the token sequence  $X = [x_1, \dots, x_T]$  of a sample as a data stream, where self-supervised learning is performed to compress visual semantics into the hidden state  $W$ . **The update rule** is written as the following gradient descent form,

$$W_t = W_{t-1} - \eta \nabla_{W_{t-1}} \ell(W_{t-1}; x_t), \quad (1)$$

and **the output rule** for the output sequence  $Z = [z_1, \dots, z_T]$  is given by,

$$z_t = f(x_t; W_t) = W_t x_t, \quad (2)$$

where  $\ell$  is the self-supervised loss,  $\eta$  is the learning rate and  $W$  could be any neural network. This adaptation occurs continuously during both training and testing, enabling the model to refine its internal representations in response to observed data patterns, thus called ‘‘Test-Time Training’’.

## 4 Vision-TTT: Vision Test-Time Training

### 4.1 TTT as a Vision Learner

**Formulation of Vision-TTT.** Analogous to the attention mechanism [51], given the input visual sequence  $X = [x_1, \dots, x_T]$ , we first project it to the key,

query and value vectors,

$$X^K, X^Q, X^V = \theta_K X, \theta_Q X, \theta_V X, \quad (3)$$

where  $\theta_K, \theta_Q, \theta_V$  are linear projection matrices. The self-supervised task can be formulated as a reconstruction problem of the original input and the target is set to minimize the  $L2$  norm loss,

$$\ell(W_{t-1}; x_t) = \|f(x_t^K, W_{t-1}) - x_t^V\|^2 = \|W_{t-1}x_t^K - x_t^V\|^2, \quad (4)$$

with the output token generated as,

$$z_t = f(x_t^Q; W_t) = W_t x_t^Q, \quad (5)$$

where  $x_t^K, x_t^Q, x_t^V$  are slices of  $X^K, X^Q, X^V$  at timestep  $t$ , respectively. This formulation can be interpreted as reconstructing the  $x_t^V$  (label view) with the projected  $x_t^K$  (training view) and querying with  $x_t^Q$  (test view) [44].

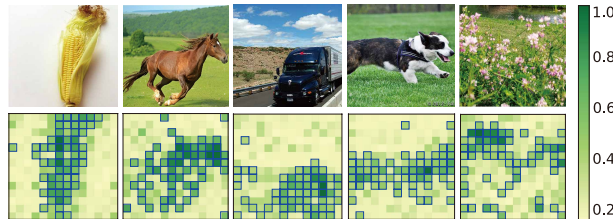


**Fig. 3:** Gradient Magnitude Map (illustrated by Eq. (6)). Vision-TTT employs gradients as the explicit indicators to quantify token semantics.

**Interpretability of Vision-TTT.** By taking the derivative of  $W_{t-1}$  in Eq. (4) with respect to the self-supervised loss  $\ell$ , we can obtain the gradient  $G_t$  to quantify the token importance at timestep  $t$ ,

$$G_t = \nabla_{W_{t-1}} \ell(W_{t-1}; x_t) = 2(W_{t-1}x_t^K - x_t^V)(x_t^K)^T. \quad (6)$$

As shown in Fig. 3, we visualize the  $G_t$  distribution on the 2D patch tokens. We observe that tokens with significant visual semantics exhibit larger gradient signal values, which means Vision-TTT has a clear understanding of different regions after training. This provides us with an inherent explainability tool, just as the attention map visualization for vision transformers.

**Efficiency of Vision-TTT.** The original token-wise TTT relies on sequential computation, and thus suffers from insufficient efficiency. To fully exploit the parallelism of modern GPUs, we reduce the hidden size from  $W \in \mathbb{R}^{D \times D}$  to  $W \in \mathbb{R}^{nh \times d \times d}$  with multi-head mechanism [51], where  $nh$  is the number of heads,  $d$  is the head dimension set to 64, and  $D = nh \times d$ . Besides, the granularity of gradient descent is changed from 1 to 16. In other words, we perform mini-batch gradient descent along the visual token sequence with mini-batch size  $b = 16$ .

The update rule within the mini-batch  $b$  then follows a causal form [26]. For instance, starting from the initial values of  $W_0$ , the hidden state at timestep  $t$  ( $0 < t \leq b$ ) within the first mini-batch is expressed as,

$$W_t = W_{t-1} - \eta G_t = W_0 - \sum_{s=1}^t G_s. \quad (7)$$

By leveraging the small matrix parallel computing capability of Tensor Cores ( $16 \times 16$ ), we achieve linear-time throughput. Referring to the great work of TTT in NLP [44], we encapsulate the forward and backward kernels with Triton [49] to transform the linear modeling capability of TTT from theory into reality. Due to space, the detailed kernel implementation is deferred to the Appendix.

## 4.2 Overall Architecture

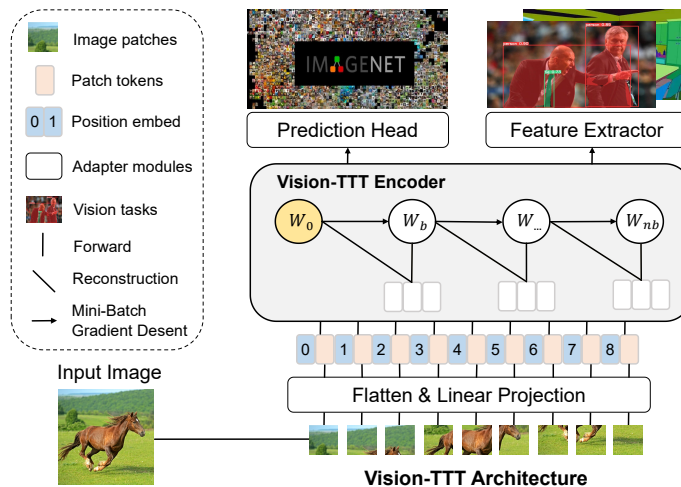


**Fig. 4:** Overall architecture of Vision-TTT. It consists of three stages: Patchification, Vision-TTT Encoder, and Task Adapters to learn representation for vision tasks.

As illustrated in Fig. 4, Vision-TTT consists of three stages as follows.

❶ **Patchification.** The input image  $I \in \mathbb{R}^{H \times W \times C}$  is split into a sequence of 1D patches  $x_p \in \mathbb{R}^{T \times (P^2 \cdot C)}$  [13, 67], where  $(H, W)$  is the resolution of the original image,  $C$  is the channel,  $P^2$  is the size of each rectangle patch and the sequence length is  $T = \frac{HW}{P^2}$ . Then a learnable projection  $E \in \mathbb{R}^{(P^2 \cdot C) \times D}$  is appended and a position embedding  $E_{\text{pos}} \in \mathbb{R}^{(T+1) \times D}$  is added to form the processed input  $y_0$  of feature embedding  $D$ ,

$$y_0 = [x_p^1 E, x_p^2 E, \dots, x_p^T E] + E_{\text{pos}}, \quad (8)$$

② **Vision-TTT Encoder.** The processed input is then fed into  $L$  hybrid blocks. Each of them consists of a **Vitttt** block and a successive **SwiGluMLP** [40], a variant of Gated Linear Units [8].

$$\begin{aligned} y'_i &= \text{Vitttt}(\text{LN}(y_{i-1})) + y_{i-1}, \\ y_i &= \text{SwiGluMLP}(\text{LN}(y'_i)) + y'_i, \end{aligned} \quad (9)$$

where LN denotes layer normalization,  $y'_i$  is the intermediate activation.

③ **Task Adapters.** During the ImageNet [9] pretraining stage, we adopt mean pool and a linear detection head to extract the class possibility  $\hat{p}$  as follows,

$$\hat{p} = \text{Linear}(\text{MeanPool}(\text{LN}(y_l))). \quad (10)$$

When finetuning for downstream COCO [29] detection and ADE20K [65] segmentation tasks, the common practice is to freeze the encoder backbone and only train the feature extractor for adaptation.

### 4.3 Design of Vitttt Block

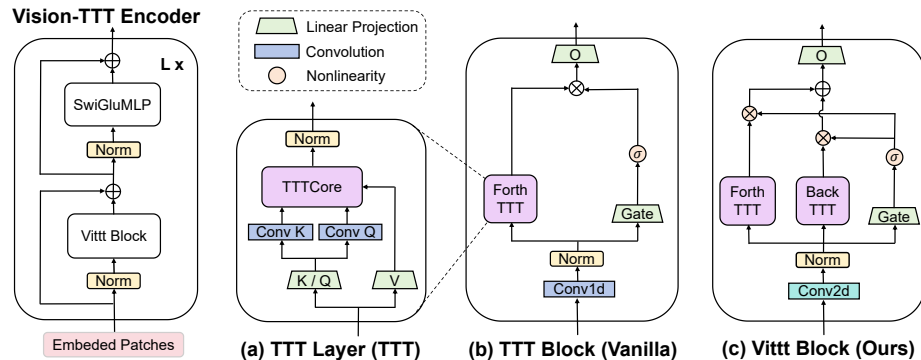


**Fig. 5: Vitttt Block.** It evolves from vanilla TTT with two 2D designs: the long-term bidirectional scan strategy and the short-term Conv2d token aggregation module.

The design route from the original TTT layer to our **Vitttt** block is illustrated in Fig. 5. The vanilla TTT block [44] is essentially a gated linear unit that introduces non-linearity to the original TTT layer. Referring to Fig. 5 (b), given the input sequence  $X$  and the output sequence  $Z$  of the **Forth TTT** module, with the non-linearity  $\sigma$  set to **GELU**, the vanilla TTT block can be formulated as,

$$Z_{\text{gated}} = \text{GELU}(\text{Linear}(X)) \odot Z. \quad (11)$$

Although the vanilla TTT block is a promising vision learner, it is originally designed for unidirectional modeling, which conflicts with 2D spatial data. To introduce spatial locality, we further integrate two 2D architectural designs.

**Bidirectional Scan.** We employ bidirectional scan to alleviate the unidirectional bias of 1D global sequence modeling [39, 67], which simultaneously correlates tokens in the forward ( $Z_{\text{forth}}$ ) and reverse ( $Z_{\text{back}}$ ) routes,

$$Z_{\text{bidir.}} = \text{GELU}(\text{Linear}(X_{\text{Conv2d}})) \odot (Z_{\text{forth}} + \text{flip}(Z_{\text{back}})). \quad (12)$$

**Conv2d Module.** The  $X_{\text{Conv2d}}$  is the pre-processed result of the 1D input sequence  $X$  to aggregate 2D local tokens. We use depth wise convolution [5] to reduce the introduced parameters (0.02M, 0.04M, 0.08M for **Vittt-T/S/B**).

$$X_{\text{Conv2d}} = \text{DWConv}(X). \quad (13)$$

The global bidirectional scan strategy to capture long-term dependency in two directions and the local Conv2d module to aggregate 2D short-term relevancy together form **Vittt** block in Fig. 5 (c) and enable adaptation to visual tasks.

## 5 Experiments

We conduct extensive vision experiments to validate the expressiveness of Vision-TTT, including ImageNet [9] classification and downstream COCO [29] detection and ADE20K [65] segmentation tasks. In addition, we also measure the FLOPs, throughput and memory consumption metrics across resolutions ranging from  $224 \times 224$  to  $1280 \times 1280$  to demonstrate Vision-TTT’s linear-time efficiency.

### 5.1 Image Classification

**Settings.** We first evaluate **Vittt** on the ImageNet-1K dataset [9] and compare its performance against the benchmarks from ViT [13], DeiT [50], and linear-complexity gMLP [30], Vision-RWKV [14], Vim [67]. The hierarchical version **Vittt-H** adopts the same downsampling strategy as SwinTransformer [33]. For fair comparison, we mainly follow the training recipe of DeiT [50] and SwinTransformer [33]. Further details are listed in Appendix.

**Main Results.** As shown in Tab. 1, **Vittt-T/S/B** achieves 77.3%, 81.2%, 82.5% Top-1 accuracy on ImageNet classification, respectively. Compared with other methods, **Vittt-T/S** has significant improvements, which is +1.2% and +0.9% better than the competitive Vim-T/S. Even for the base size model, **Vittt-B** surpasses its counterparts DeiT-B, gMLP-B, VRWKV-B and Vim-B by +0.5% ~ +0.9%, demonstrating the strong expressiveness of Vision-TTT at scale. Notably, such advantages can be seamlessly transferred to hierarchical architectures.

### 5.2 Downstream Tasks

**Settings.** We benchmark **Vittt** model against other popular non-hierarchical visual sequence modeling methods, including ViT [13], Vision-RWKV [14] and Vim [67]. For object detection and instance segmentation, we evaluate **Vittt** on the COCO2017 dataset [29]. The procedure mainly follows the Vision-RWKV recipe [14] to integrate the ViT-Adapter [4] and Mask-RCNN [21] detection head

**Table 1:** Performance comparison on ImageNet-1K classification. We report the parameters (#Param.), FLOPs and Top-1 Accuracy (%) metrics. *Left:* non-hierarchical architectures; *Right:* hierarchical architectures.

Method	size	#Param.	FLOPs	Acc.	Method	size	#Param.	FLOPs	Acc.
<b>Transformers</b>					<b>CNNs</b>				
ViT-B/16	384 <sup>2</sup>	86M	55.4G	77.9	RegNetY-4G	224 <sup>2</sup>	12M	4G	80.0
ViT-L/16	384 <sup>2</sup>	307M	190.7G	76.5	RegNetY-8G	224 <sup>2</sup>	25M	8G	81.7
DeiT-T	224 <sup>2</sup>	6M	1.3G	72.2	RegNetY-16G	224 <sup>2</sup>	45M	16G	82.9
DeiT-S	224 <sup>2</sup>	22M	4.6G	79.8	EffNet-B3	300 <sup>2</sup>	12M	1.8G	81.6
DeiT-B	224 <sup>2</sup>	86M	17.6G	81.8	EffNet-B4	380 <sup>2</sup>	19M	4.2G	82.9
<b>MLPs</b>					EffNet-B5	456 <sup>2</sup>	30M	9.9G	83.6
gMLP-T	224 <sup>2</sup>	6M	1.4G	72.3	ConvNeXt-T	224 <sup>2</sup>	29M	4.5G	82.1
gMLP-S	224 <sup>2</sup>	20M	4.5G	79.6	ConvNeXt-S	224 <sup>2</sup>	50M	8.7G	83.1
gMLP-B	224 <sup>2</sup>	73M	15.8G	81.6	ConvNeXt-B	224 <sup>2</sup>	89M	15.4G	83.8
<b>RWKVs</b>					<b>Transformers</b>				
VRWKV-T	224 <sup>2</sup>	6M	1.2G	75.1	Swin-T	224 <sup>2</sup>	28M	4.5G	81.3
VRWKV-S	224 <sup>2</sup>	24M	4.6G	80.1	Swin-S	224 <sup>2</sup>	50M	8.7G	83.0
VRWKV-B	224 <sup>2</sup>	94M	18.2G	82.0	Swin-B	224 <sup>2</sup>	88M	15.4G	83.5
<b>SSMs</b>					<b>SSMs</b>				
Vim-T	224 <sup>2</sup>	7M	1.5G	76.1	VMamba-T	224 <sup>2</sup>	30M	4.9G	82.5
Vim-S	224 <sup>2</sup>	26M	5.2G	80.3	VMamba-S	224 <sup>2</sup>	50M	8.7G	83.6
Vim-B	224 <sup>2</sup>	98M	18.8G	81.9	VMamba-B	224 <sup>2</sup>	89M	15.4G	83.9
<b>TTTs</b>					<b>TTTs</b>				
Vittt-T	224 <sup>2</sup>	6M	1.4G	<b>77.3</b>	Vittt-H-T	224 <sup>2</sup>	28M	5.6G	<b>82.6</b>
Vittt-S	224 <sup>2</sup>	22M	5.3G	<b>81.2</b>	Vittt-H-S	224 <sup>2</sup>	50M	10.8G	<b>83.8</b>
Vittt-B	224 <sup>2</sup>	87M	20.3G	<b>82.5</b>	Vittt-H-B	224 <sup>2</sup>	88M	18.8G	<b>84.2</b>

on our plain Vittt models. The image resolution is scaled up to  $1333 \times 800$ . In addition, we perform semantic segmentation on the ADE20K dataset [65]. For a fair comparison, we also follow prior works Vim [67] and Vision-RWKV [14] to use UperNet [57] as the segmentation head. All images are cropped into  $512 \times 512$ . The training details are provided in Appendix.

**Main Results.** Tab. 2 demonstrates the remarkable superiority of Vision-TTT on dense prediction tasks. Vittt-T outperforms the strongest baseline Vim-T by +0.4% AP<sup>b</sup>, +0.4% AP<sup>m</sup> and +0.2% mIoU. The advantage is further enlarged to +1.0% AP<sup>b</sup>, +1.1% AP<sup>m</sup> and +0.7% mIoU for Vittt-S against Vim-S. For the base size model, where Vim-B fails to scale effectively, Vittt-B still maintains consistent performance gains of +1.0% AP<sup>b</sup>, +1.1% AP<sup>m</sup> and +0.2% mIoU over its best counterpart VRWKV-B. Note that the performance superiority is more significant on COCO detection ( $1333 \times 800$  resolution, i.e. 4200 image tokens) than on ADE20K segmentation ( $512 \times 512$  resolution, i.e. 1024 image tokens)

**Table 2:** Performance comparison on downstream COCO2017 detection (*Left*) and ADE20K segmentation (*Right*) tasks. We report the parameters (#Param.), FLOPs and AP<sup>b</sup>, AP<sup>m</sup>, mIoU metrics, respectively. FLOPs are calculated with  $1333 \times 800$  resolution for detection and  $512 \times 512$  resolution for segmentation tasks. ViT-T<sup>†</sup> is the shifted window version [33] of ViT [13] to trade off some accuracy for linear complexity.

Method	#Param.	FLOPs	AP <sup>b</sup>	AP <sup>m</sup>	Method	#Param.	FLOPs	mIoU
ViT-T <sup>†</sup>	8M	95.4G	41.1	37.5	ViT-T <sup>†</sup>	8M	23.2G	42.4
ViT-T	8M	147.1G	41.6	37.9	ViT-T	8M	20.9G	42.6
VRWKV-T	8M	67.9G	41.7	38.0	VRWKV-T	8M	16.6G	43.3
Vim-T	9M	76.7G	41.8	38.2	Vim-T	9M	18.4G	43.4
<b>Vittt-T</b>	8M	74.3G	<b>42.2</b>	<b>38.6</b>	<b>Vittt-T</b>	8M	17.8G	<b>43.6</b>
ViT-S <sup>†</sup>	28M	241.2G	44.6	39.7	ViT-S <sup>†</sup>	28M	58.8G	45.8
ViT-S	28M	344.5G	44.9	40.1	ViT-S	28M	54.0G	46.2
VRWKV-S	29M	189.9G	44.8	40.2	VRWKV-S	29M	46.3G	47.2
Vim-S	32M	203.6G	44.9	40.2	Vim-S	32M	49.7G	47.4
<b>Vittt-S</b>	28M	206.3G	<b>45.9</b>	<b>41.3</b>	<b>Vittt-S</b>	28M	50.3G	<b>48.1</b>
ViT-B <sup>†</sup>	100M	686.7G	46.2	41.5	ViT-B <sup>†</sup>	100M	167.5G	48.4
ViT-B	100M	893.3G	46.8	41.8	ViT-B	100M	157.9G	48.8
VRWKV-B	107M	599.0G	46.8	41.7	VRWKV-B	107M	146.0G	49.2
Vim-B	111M	611.5G	46.6	41.6	Vim-B	111M	149.2G	48.9
<b>Vittt-B</b>	100M	646.7G	<b>48.0</b>	<b>42.8</b>	<b>Vittt-B</b>	100M	157.7G	<b>49.4</b>

task, which validates the powerful expressiveness of Vision-TTT for even longer sequence modeling tasks.

### 5.3 Efficiency Analysis

**Settings.** Throughput is assessed on a 48G L40S GPU paired with an AMD EPYC 7763 CPU, utilizing the toolkit provided by [56]. Following [33], we set the batch size to 64 to test the FPS (frames per second) and memory footprint.

**Computational Efficiency.** Given an input sequence  $y \in \mathbb{R}^{1 \times T \times D}$ , the theoretical computation complexity is given by,

$$\begin{aligned}
 \Omega(\text{ViT}) &= 4TD^2 + 2T^2D \\
 \Omega(\text{Vim}) &= 6TD^2 + 18T(2D)N \\
 \Omega(\text{Vittt}) &= 6TD^2 + 6Tdd + 4bTD,
 \end{aligned} \tag{14}$$

where  $b = 16$  denotes the mini-batch size,  $d = 64$  is the head dimension, and  $N = 16$  is the state expansion factor of Mamba [18]. By referring to Vim [67], we include the input/output projections, the discretization steps, the gating operations and then multiply the bidirectional factor to compute the overall complexity of Vim blocks. Obviously, ViT exhibits quadratic complexity w.r.t. the sequence length  $T$ . In contrast, both Vim and Vittt enjoy linear complexity via RNN-style updates, enabling efficient long-sequence modeling. As shown in

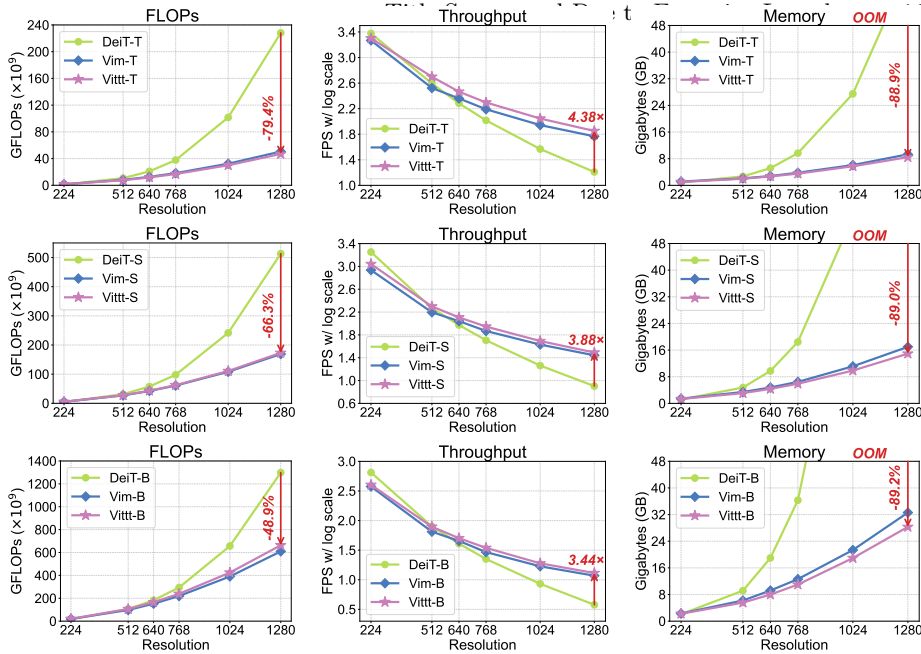


**Fig. 6:** Efficiency comparison between DeiT [50], Vim [67] and our Vitti model. We sketch the FLOPs, throughput, and memory footprint curves for different resolutions ranging from  $224 \times 224$  (i.e. 196 tokens) to  $1280 \times 1280$  (i.e. 6400 tokens).

the left two columns of Fig. 6, the linearly increasing FLOPs and throughput of Vitti align well with the theoretical complexity analysis. Although DeiT achieves slightly higher throughput in processing  $224 \times 224$  images, it slows down quickly with the growth of resolution. At  $1280 \times 1280$  resolution, Vitti-T/S/B saves 79.4%, 66.3%, 48.9% FLOPs and achieves  $4.38\times$ ,  $3.88\times$ ,  $3.44\times$  higher FPS than DeiT-T/S/B, respectively. For the linear models Vitti and Vim, Vitti-T has fewer FLOPs than Vim-T, but Vitti-S/B yield slightly more FLOPs than Vim-S/B, implying that Vitti has a larger constant coefficient related to the embedding size  $D$ . Nevertheless, we observe that Vitti consistently outperforms Vim in speed across different model sizes and input resolutions. This stems from their distinct kernel utilization strategies during execution. While Vim relies on the selective scan mechanism [18] parallelized over CUDA Cores, Vitti directly operates on Tensor Cores, which are  $16 \times 16$  specialized matrix multiplication units that runs several to tens of times faster.

**Memory Efficiency.** With the global batch size of  $B$ , the asymptotic memory complexity is as follows,

$$\begin{aligned}
 \Omega(\text{ViT}) &= \mathcal{O}(BTD + BT^2) \\
 \Omega(\text{Vim}) &= \mathcal{O}(BTD + BTDN) \\
 \Omega(\text{Vitti}) &= \mathcal{O}(BTD + BTd + BTdd/b).
 \end{aligned} \tag{15}$$

Linear models of Vim and Vitti alleviate the quadratic memory cost w.r.t.  $T$  that ViT demands. Our implementation follows Mamba [18] to incorporate kernel fusion and recomputation techniques, which further reduces the mem-

ory footprint to  $\mathcal{O}(BTD)$ . As shown in the right column of Fig. 6, while the memory consumption of DeiT explodes at high resolutions, the footprint only grows linearly for Vim and **Vittt**. At  $1280 \times 1280$  resolution, **Vittt**-T/S/B consumes approximately 89.0% less memory than DeiT-T/S/B. We also observe a considerable memory reduction of **Vittt**-S/B compared to Vim-S/B beyond  $1024 \times 1024$  resolution, indicating that **Vittt** enjoys a smaller constant factor of memory usage than Vim.

The above experiments consistently demonstrate the linear-complexity computation and memory consumption of Vision-TTT across diverse model scales and sequence lengths. This effectively bypasses the scalability bottleneck of Vision Transformers and renders it highly favorable for high-resolution modeling. For readers with further interest in Vision-TTT’s efficiency, we provide the derivation of the computational complexity, the hardware-aware implementation, and additional insights into the memory I/O optimization in the Appendix.

#### 5.4 Ablation Study

To verify the effectiveness of our design, we systematically explore the design space to identify favorable configurations. Specifically, 1) we conduct ablation studies on the inner modules of the **Vittt** block to validate the rationality of our architecture design; 2) we experiment with different classification strategies to obtain the most compatible supervised learning scheme; 3) we also compare different numbers of learnable initial states  $W_0 \in \mathbb{R}^{nh \times d \times d}$  in bidirectional scanning. The results demonstrate that our design for Vision-TTT is modularly effective, friendly to supervised learning, and achieves a favorable trade-off between model parameters and performance.

**Table 3:** Performance comparison for different snapshot on the design route for **Vittt**-T. Throughput metric FPS (frames per second) is tested with batch size 64.

Design Route	#Param.	FLOPs	FPS	Top-1 Acc.	AP <sup>b</sup>	AP <sup>m</sup>	mIoU
TTT layer	5.43M	1.07G	3892	73.8	40.4	36.5	41.5
+ gating	5.89M	1.15G	3565	75.0	41.2	37.1	42.2
+ Conv1d (vanilla)	5.90M	1.16G	3246	75.4	41.3	37.6	42.8
+ bidir.	5.90M	1.42G	2068	76.9	42.0	38.2	43.3
+ Conv2d ( <b>Vittt</b> )	5.91M	1.44G	2029	77.3	42.2	38.6	43.6

**Design Route of Vittt Block.** The design route in Tab. 3 follows the illustration in Sec. 4.3. From the TTT layer to the vanilla TTT, the gating mechanism and Conv1d module is incorporated, endowing TTT with nonlinearity and unidirectional token perception. This process incurs a 16.6% drop in model throughput, while bringing preliminary gains for +1.6% in classification accuracy, +0.9% AP<sup>b</sup>, +1.1% AP<sup>m</sup> for detection and +1.3% mIoU for segmentation. To form our **Vittt** block for 2D vision data, the bidirectional strategy and the Conv2d module are successively applied, only introducing  $\sim 0.02$ M parameters. Although the FPS metric reduces by 37.5%, results show that the 2D design of

**Vittt** block is completely worthwhile for further improvement of performance metrics by +1.9% for classification, +0.9% AP<sup>b</sup>, +1.0% AP<sup>m</sup> for detection and +0.8% mIoU for segmentation, respectively.

**Table 4:** Performance comparison for different classification strategies on **Vittt-T**.

Method	#Param.	FLOPs	Top-1 Acc.	AP <sup>b</sup>	AP <sup>m</sup>	mIoU
HeadClassTok	6M	1.4G	76.4	41.6	37.8	43.0
MidClassTok	6M	1.4G	76.6	41.7	37.9	43.0
DoubleClassTok	6M	1.4G	75.2	41.0	37.2	42.5
MaxPool	6M	1.4G	77.0	42.0	38.3	43.4
MeanPool	6M	1.4G	77.3	42.2	38.6	43.6

**Ablation of Classification Strategy.** Following Vim [67], we experiment with five different ways to obtain the classification feature to identify the optimal scheme for class-supervised learning. The head class token [13] refers to insert an extra token before the input patch sequence and using only this token after the output layer to compute the class possibilities. The “MidClassTok” and “DoubleClassTok” are two variants to insert one class token in the middle or two class tokens before and after the input patch sequence [67], respectively. “MaxPool” and “MeanPool” are two pooling strategies that extract the  $L2$ -norm maximum or the average of the output feature sequence. As shown in Tab. 4, the two pooling strategies achieve significantly better performance than the other three class token strategies. Between the two pooling strategies, the “MeanPool” strategy is the more suitable for the gradient-driven representation of Vision-TTT, outperforming “MaxPool” by +0.3% in classification accuracy, +0.2% AP<sup>b</sup>, +0.3% AP<sup>m</sup> for detection and +0.2% mIoU for segmentation.

**Table 5:** Performance comparison for different numbers of learnable initial states. The superscript numbers of  $W_0^0$ ,  $W_0^1$ ,  $W_0^2$  denote the learnable number of the two initial states  $W_0$  in bidirectional scanning process.

Method	#Param.	FLOPs	Top-1 Acc.	AP <sup>b</sup>	AP <sup>m</sup>	mIoU
Vittt- $W_0^0$ -T	5M	1.4G	76.9	41.9	38.2	43.3
Vittt- $W_0^1$ -T	6M	1.4G	77.3	42.2	38.6	43.6
Vittt- $W_0^2$ -T	7M	1.4G	77.5	42.4	38.7	43.8
Vittt- $W_0^0$ -S	18M	5.3G	80.8	45.2	40.5	47.4
Vittt- $W_0^1$ -S	22M	5.3G	81.2	45.9	41.3	48.1
Vittt- $W_0^2$ -S	26M	5.3G	81.6	46.3	41.4	48.3
Vittt- $W_0^0$ -B	72M	20.3G	82.0	47.2	42.5	48.8
Vittt- $W_0^1$ -B	87M	20.3G	82.5	48.0	42.8	49.4
Vittt- $W_0^2$ -B	102M	20.3G	82.6	48.1	43.0	49.5

**Number of Learnable Initial States.** Recall that in Sec. 4.3 we adopt bidirectional scan strategy to model the long-term dependency of 2D spatial data.

In the process there are two initial states  $W_0 \in \mathbb{R}^{nh \times d \times d}$  in **Forth TTT** and **Back TTT** modules. Under such a scenario, the initialization of the hidden states is a noteworthy problem [44]. Unlike general parameter initialization, these states can either be initialized once before training, or set as learnable parameters and trained during supervised learning (surely introduces trainable parameters). We denote the one-time initialization before training as  $\text{Vittt-}W_0^0$ , where no hidden states are learnable. The setting  $\text{Vittt-}W_0^2$  uses two separate learnable initial states for **Forth TTT** and **Back TTT**, and  $\text{Vittt-}W_0^1$  shares one copy of learnable initial state across both scanning directions. As shown in Fig. 5, more learnable initial states generally reduces interference between different scanning paths and leads to improved performance. Although  $\text{Vittt-}W_0^2$  achieves the highest performance, it introduces considerable additional parameters than its counterparts **DeiT** [50], **Vim** [67] and **Vision-RWKV** [14]. We therefore set  $\text{Vittt-}W_0^1$  as the default configuration to to balance the model parameters and the performance.

## 6 Visualization of Interpretability

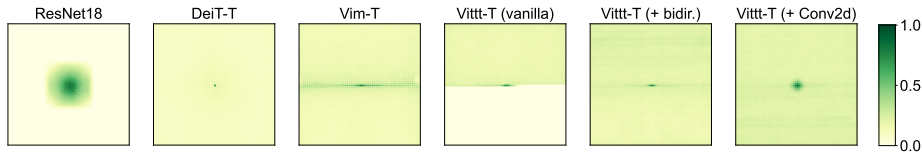


**Fig. 7:** Comparison of Effective Receptive Field (ERF) [35]. Pixels with higher intensity indicate larger responses related to the central pixel.

**Effective Receptive Field (ERF).** The Effective Receptive Field (ERF) [11, 35] refers to the region in the input space that contributes to the activations of a specific output unit. As shown in Fig. 7, we conduct a comparative analysis of the central pixel’s ERF across various visual backbones, including **ResNet** [22], **DeiT** [50], **Vim** [67] and three snapshots of **Vittt** illustrated in Sec. 5.4. From the “vanilla” version to the “+bidir.” version, **Vittt** overcomes the limitations of unidirectional modeling. Further based on the bidirectional scan strategy, the “+Conv2d” version ultimately exhibits the globally radial pattern, demonstrating the effectiveness of our design route in Sec. 4.3. In addition, we observe that **DeiT**, **Vim**, **Vittt** all achieve global coverage of the pixels, but the 2D-aware distribution of **Vittt** may intuitively explain its superior expressiveness.

**Gradient Magnitude Map.** Similar to the attention maps [51] for Vision Transformers and the activation maps [32] for Vision Mambas, there are also intermediate features to gain an in-depth understanding of Vision-TTT’s representation. As shown in Fig. 8, we visualize the Gradient Magnitude Map (GMM) of Vision-TTT before and after training and observe that Vision-TTT develops a discriminative understanding of different input regions. Before training, while the network initialization may partially outline the edges of the main objects, the gradient distribution remains relatively uniform without focusing on specific parts. After supervised learning with target class labels, Vision-TTT

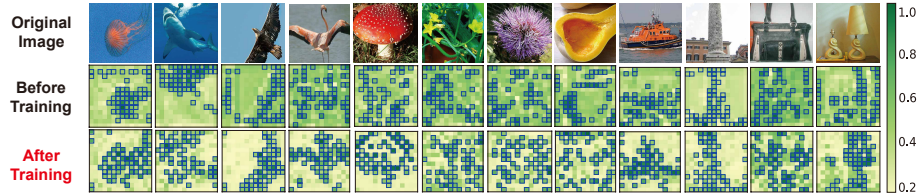


**Fig. 8:** Gradient Magnitude Map of **Vttt-T** before and after training. Tokens with higher intensity indicate steeper gradients (Eq. (6)) and greater token importance.

prominently highlights the regions with dense visual semantics and diminishes its attention to irrelevant background regions. The GMM serves as a unique interpretive tool for Vision-TTT, offering patch-level explanatory insights that may lay a foundation for future academic advancements of Vision-TTT.

## 7 Conclusion

In this paper, we propose Vision-TTT that introduces a novel sequence modeling method Test-Time Training to the visual representation learning domain. Our method addresses the inherent limitations of Vision Transformers by maintaining a globally radial receptive field meanwhile keeping linear complexity. To adapt the unidirectional TTT model for 2D vision tasks, we propose to utilize bidirectional scan strategy to capture long-term dependency and Conv2d module for short-term token aggregation in **Vttt** blocks. In addition, we integrate kernel implementation for Vision-TTT with linear-complexity parallelism. The significant performance of **Vttt** across various vision tasks at different model scales, and the verified efficiency for higher resolution images, together demonstrate it as a strong candidate for the next-generation generic visual backbone.

## References

1. Andrychowicz, M., Denil, M., Colmenarejo, S.G., Hoffman, M.W., Pfau, D., Schaul, T., de Freitas, N.: Learning to learn by gradient descent by gradient descent. In: Neural Information Processing Systems (2016)
2. Chen, C.F.R., Fan, Q., Panda, R.: Crossvit: Cross-attention multi-scale vision transformer for image classification. In: 2021 IEEE/CVF International Conference on Computer Vision (ICCV). pp. 347–356 (2021)
3. Chen, T., Ye, Z., Tan, Z., Gong, T., Wu, Y., Chu, Q., Liu, B., Yu, N., Ye, J.: Mimi-istd: Mamba-in-mamba for efficient infrared small-target detection. IEEE Transactions on Geoscience and Remote Sensing (2024)
4. Chen, Z., Duan, Y., Wang, W., He, J., Lu, T., Dai, J., Qiao, Y.: Vision transformer adapter for dense predictions. arXiv preprint arXiv:2205.08534 (2022)
5. Chollet, F.: Xception: Deep learning with depthwise separable convolutions. In: 2017 IEEE Conference on Computer Vision and Pattern Recognition (CVPR). pp. 1800–1807 (2017)

6. Dai, Z., Liu, H., Le, Q.V., Tan, M.: Coatnet: Marrying convolution and attention for all data sizes. *Advances in neural information processing systems* pp. 3965–3977 (2021)
7. Dao, T., Gu, A.: Transformers are SSMS: Generalized models and efficient algorithms through structured state space duality. In: *International Conference on Machine Learning (ICML)* (2024)
8. Dauphin, Y.N., Fan, A., Auli, M., Grangier, D.: Language modeling with gated convolutional networks (2017)
9. Deng, J., Dong, W., Socher, R., Li, L.J., Li, K., Fei-Fei, L.: Imagenet: A large-scale hierarchical image database. *2009 IEEE Conference on Computer Vision and Pattern Recognition* pp. 248–255 (2009)
10. Ding, M., Xiao, B., Codella, N.C.F., Luo, P., Wang, J., Yuan, L.: Davit: Dual attention vision transformers. In: *European Conference on Computer Vision* (2022)
11. Ding, X., Zhang, X., Han, J., Ding, G.: Scaling up your kernels to  $31 \times 31$ : Revisiting large kernel design in cnns. In: *2022 IEEE/CVF Conference on Computer Vision and Pattern Recognition (CVPR)*. pp. 11953–11965 (2022)
12. Dong, X., Bao, J., Chen, D., Zhang, W., Yu, N., Yuan, L., Chen, D., Guo, B.: Cswin transformer: A general vision transformer backbone with cross-shaped windows. *2022 IEEE/CVF Conference on Computer Vision and Pattern Recognition (CVPR)* pp. 12114–12124 (2021)
13. Dosovitskiy, A., Beyer, L., Kolesnikov, A., Weissenborn, D., Zhai, X., Unterthiner, T., Dehghani, M., Minderer, M., Heigold, G., Gelly, S., Uszkoreit, J., Houslyby, N.: An image is worth 16x16 words: Transformers for image recognition at scale. *ICLR* (2021)
14. Duan, Y., Wang, W., Chen, Z., Zhu, X., Lu, L., Lu, T., Qiao, Y., Li, H., Dai, J., Wang, W.: Vision-rwkv: Efficient and scalable visual perception with rwkv-like architectures. *arXiv preprint arXiv:2403.02308* (2024)
15. Fukushima, K.: Neocognitron: A self-organizing neural network model for a mechanism of pattern recognition unaffected by shift in position. *Biological Cybernetics* (1980)
16. Gandelsman, Y., Sun, Y., Chen, X., Efros, A.: Test-time training with masked autoencoders. *Advances in Neural Information Processing Systems* (2022)
17. Gao, P., Lu, J., Li, H., Mottaghi, R., Kembhavi, A.: Container: Context aggregation network. *arXiv preprint arXiv:2106.01401* (2021)
18. Gu, A., Dao, T.: Mamba: Linear-time sequence modeling with selective state spaces. In: *First conference on language modeling* (2024)
19. Gu, A., Goel, K., Ré, C.: Efficiently modeling long sequences with structured state spaces. *arXiv preprint arXiv:2111.00396* (2021)
20. Hatamizadeh, A., Kautz, J.: Mambavision: A hybrid mamba-transformer vision backbone. In: *Proceedings of the Computer Vision and Pattern Recognition Conference*. pp. 25261–25270 (2025)
21. He, K., Gkioxari, G., Dollár, P., Girshick, R.B.: Mask r-cnn (2017)
22. He, K., Zhang, X., Ren, S., Sun, J.: Deep residual learning for image recognition. In: *2016 IEEE Conference on Computer Vision and Pattern Recognition (CVPR)*. pp. 770–778 (2016)
23. Hochreiter, S., Schmidhuber, J.: Long short-term memory. *Neural Computation* **9**, 1735–1780 (1997)
24. Huang, G., Liu, Z., Van Der Maaten, L., Weinberger, K.Q.: Densely connected convolutional networks. In: *2017 IEEE Conference on Computer Vision and Pattern Recognition (CVPR)*. pp. 2261–2269 (2017)

25. Huang, T., Pei, X., You, S., Wang, F., Qian, C., Xu, C.: Localmamba: Visual state space model with windowed selective scan. In: ECCV Workshops (2024)
26. Katharopoulos, A., Vyas, A., Pappas, N., Fleuret, F.: Transformers are rnns: Fast autoregressive transformers with linear attention. In: International Conference on Machine Learning (2020)
27. Krizhevsky, A., Sutskever, I., Hinton, G.E.: Imagenet classification with deep convolutional neural networks. *Communications of the ACM* (2012)
28. Liao, B., Wang, X., Zhu, L., Zhang, Q., Huang, C.: Vig: Linear-complexity visual sequence learning with gated linear attention. In: Proceedings of the AAAI Conference on Artificial Intelligence (2025)
29. Lin, T.Y., Maire, M., Belongie, S.J., Hays, J., Perona, P., Ramanan, D., Dollár, P., Zitnick, C.L.: Microsoft coco: Common objects in context. In: European Conference on Computer Vision (2014)
30. Liu, H., Dai, Z., So, D.R., Le, Q.V.: Pay attention to mlps. In: Neural Information Processing Systems (2021)
31. Liu, S., Chen, T., Chen, X., Chen, X., Xiao, Q., Wu, B., Kärkkäinen, T., Pechenizkiy, M., Mocanu, D., Wang, Z.: More convnets in the 2020s: Scaling up kernels beyond 51x51 using sparsity. arXiv preprint arXiv:2207.03620 (2022)
32. Liu, Y., Tian, Y., Zhao, Y., Yu, H., Xie, L., Wang, Y., Ye, Q., Jiao, J., Liu, Y.: Vmamba: Visual state space model. *Advances in neural information processing systems* (2024)
33. Liu, Z., Lin, Y., Cao, Y., Hu, H., Wei, Y., Zhang, Z., Lin, S., Guo, B.: Swin transformer: Hierarchical vision transformer using shifted windows. 2021 IEEE/CVF International Conference on Computer Vision (ICCV) pp. 9992–10002 (2021)
34. Liu, Z., Mao, H., Wu, C.Y., Feichtenhofer, C., Darrell, T., Xie, S.: A convnet for the 2020s. In: 2022 IEEE/CVF Conference on Computer Vision and Pattern Recognition (CVPR). pp. 11966–11976 (2022)
35. Luo, W., Li, Y., Urtasun, R., Zemel, R.: Understanding the effective receptive field in deep convolutional neural networks. *Advances in neural information processing systems* (2016)
36. Pei, X., Huang, T., Xu, C.: Efficientvmamba: Atrous selective scan for light weight visual mamba. In: Proceedings of the AAAI conference on artificial intelligence (2025)
37. Peng, B., Alcaide, E., Anthony, Q., Albalak, A., Arcadinho, S., Biderman, S., Cao, H., Cheng, X., Chung, M., Derczynski, L., et al.: Rwkv: Reinventing rnns for the transformer era. In: Findings of the association for computational linguistics: EMNLP 2023. pp. 14048–14077 (2023)
38. Radford, A., Kim, J.W., Hallacy, C., Ramesh, A., Goh, G., Agarwal, S., Sastry, G., Askell, A., Mishkin, P., Clark, J., Krueger, G., Sutskever, I.: Learning transferable visual models from natural language supervision. In: International Conference on Machine Learning (2021)
39. Schuster, M., Paliwal, K.: Bidirectional recurrent neural networks. *Signal Processing, IEEE Transactions on* pp. 2673 – 2681 (12 1997)
40. Shazeer, N.: Glu variants improve transformer. arXiv preprint arXiv:2002.05202 (2020)
41. Sim'eon, O., Vo, H.V., Seitzer, M., Baldassarre, F., Oquab, M., Jose, C., Khalidov, V., Szafraniec, M., Yi, S., Ramamonjisoa, M., Massa, F., Haziza, D., Wehrstedt, L., Wang, J., Darcet, T., Moutakanni, T., Sentana, L., Roberts, C., Vedaldi, A., Tolan, J., Brandt, J., Couprie, C., Mairal, J., J'egou, H., Labatut, P., Bojanowski, P.: Dinov3 (2025)

42. Simonyan, K., Zisserman, A.: Very deep convolutional networks for large-scale image recognition. arXiv preprint arXiv:1409.1556 (2014)
43. Sun, Y., Li, X., Dalal, K., Hsu, C., Koyejo, S., Guestrin, C., Wang, X., Hashimoto, T., Chen, X.: Learning to (learn at test time). arXiv preprint arXiv:2310.13807 (2023)
44. Sun, Y., Li, X., Dalal, K., Xu, J., Vikram, A., Zhang, G., Dubois, Y., Chen, X., Wang, X., Koyejo, S., et al.: Learning to (learn at test time): Rnns with expressive hidden states. arXiv preprint arXiv:2407.04620 (2024)
45. Sun, Y., Wang, X., Liu, Z., Miller, J., Efros, A.A., Hardt, M.: Test-time training with self-supervision for generalization under distribution shifts. In: International Conference on Machine Learning (2019)
46. Tan, M., Le, Q.: Efficientnet: Rethinking model scaling for convolutional neural networks. In: International conference on machine learning. pp. 6105–6114. PMLR (2019)
47. Tan, M., Le, Q.V.: Efficientnetv2: Smaller models and faster training. In: International Conference on Machine Learning (2021)
48. Tian, Y., Xie, L., Wang, Z., Wei, L., Zhang, X., Jiao, J., Wang, Y., Tian, Q., Ye, Q.: Integrally pre-trained transformer pyramid networks. 2023 IEEE/CVF Conference on Computer Vision and Pattern Recognition (CVPR) pp. 18610–18620 (2023)
49. Tillet, P., Kung, H.T., Cox, D.D.: Triton: an intermediate language and compiler for tiled neural network computations. Proceedings of the 3rd ACM SIGPLAN International Workshop on Machine Learning and Programming Languages (2019)
50. Touvron, H., Cord, M., Douze, M., Massa, F., Sablayrolles, A., Jégou, H.: Training data-efficient image transformers & distillation through attention. In: International Conference on Machine Learning (2020)
51. Vaswani, A., Shazeer, N., Parmar, N., Uszkoreit, J., Jones, L., Gomez, A.N., Kaiser, L., Polosukhin, I.: Attention is all you need. In: Proceedings of the 31st International Conference on Neural Information Processing Systems. p. 6000–6010. NIPS'17, Curran Associates Inc., Red Hook, NY, USA (2017)
52. Wang, J., Sun, K., Cheng, T., Jiang, B., Deng, C., Zhao, Y., Liu, D., Mu, Y., Tan, M., Wang, X., Liu, W., Xiao, B.: Deep high-resolution representation learning for visual recognition. IEEE Transactions on Pattern Analysis and Machine Intelligence (2021)
53. Wang, R., Sun, Y., Tandon, A., Gandelsman, Y., Chen, X., Efros, A.A., Wang, X.: Test-time training on video streams. Journal of Machine Learning Research (2025)
54. Wang, W., Dai, J., Chen, Z., Huang, Z., Li, Z., Zhu, X., Hu, X., Lu, T., Lu, L., Li, H., Wang, X., Qiao, Y.: Internimage: Exploring large-scale vision foundation models with deformable convolutions. 2023 IEEE/CVF Conference on Computer Vision and Pattern Recognition (CVPR) pp. 14408–14419 (2022)
55. Wang, W., Xie, E., Li, X., Fan, D.P., Song, K., Liang, D., Lu, T., Luo, P., Shao, L.: Pyramid vision transformer: A versatile backbone for dense prediction without convolutions. 2021 IEEE/CVF International Conference on Computer Vision (ICCV) pp. 548–558 (2021)
56. Wightman, R.: Pytorch image models. <https://github.com/rwightman/pytorch-image-models> (2019)
57. Xiao, T., Liu, Y., Zhou, B., Jiang, Y., Sun, J.: Unified perceptual parsing for scene understanding. In: Proceedings of the European conference on computer vision (ECCV). pp. 418–434 (2018)
58. Xie, S., Girshick, R., Dollár, P., Tu, Z., He, K.: Aggregated residual transformations for deep neural networks. In: 2017 IEEE Conference on Computer Vision and Pattern Recognition (CVPR). pp. 5987–5995 (2017)

59. Xu, J.: Med-ttt: Vision test-time training model for medical image segmentation. arXiv preprint arXiv:2410.02523 (2024)
60. Xu, J., Pan, Y., Pan, X., Hoi, S.C.H., Yi, Z., Xu, Z.: Regnet: Self-regulated network for image classification. *IEEE Transactions on Neural Networks and Learning Systems* (2021)
61. Yang, C., Chen, Z., Espinosa, M., Ericsson, L., Wang, Z., Liu, J., Crowley, E.J.: Plainmamba: Improving non-hierarchical mamba in visual recognition. arXiv preprint arXiv:2403.17695 (2024)
62. Yang, S., Wang, B., Shen, Y., Panda, R., Kim, Y.: Gated linear attention transformers with hardware-efficient training. arXiv preprint arXiv:2312.06635 (2023)
63. Yuan, L., Chen, Y., Wang, T., Yu, W., Shi, Y., Tay, F.E.H., Feng, J., Yan, S.: Tokens-to-token vit: Training vision transformers from scratch on imagenet. 2021 *IEEE/CVF International Conference on Computer Vision (ICCV)* pp. 538–547 (2021)
64. Zhang, X., Tian, Y., Xie, L., Huang, W., Dai, Q., Ye, Q., Tian, Q.: Hivit: A simpler and more efficient design of hierarchical vision transformer. In: *International Conference on Learning Representations* (2023)
65. Zhou, B., Zhao, H., Puig, X., Fidler, S., Barriuso, A., Torralla, A.: Semantic understanding of scenes through the ade20k dataset. *International Journal of Computer Vision* (2016)
66. Zhou, D., Kang, B., Jin, X., Yang, L., Lian, X., Jiang, Z., Hou, Q., Feng, J.: Deepvit: Towards deeper vision transformer. arXiv preprint arXiv:2103.11886 (2021)
67. Zhu, L., Liao, B., Zhang, Q., Wang, X., Liu, W., Wang, X.: Vision mamba: Efficient visual representation learning with bidirectional state space model. In: *International Conference on Machine Learning* (2024)